THE LUNAR GLOBAL TOPOGRAPHY BY THE LASER ALTIMETER (LALT) ONBOARD KAGUYA (SELENE): RESULTS FROM THE ONE YEAR OBSERVATION. H. Araki[1], S. Tazawa[1], H. Noda[1], Y. Ishihara[1], S. Goossens[1], N. Kawano[1], S. Sasaki[1], I. Kamiya[2], H. Otake[3], J. Oberst[4], and C. K. Shum[5],[1]National Astronomical Observatory of Japan (2-12 Hoshigaoka, Ohshu Iwate, 023-0861, Japan; arakih@miz.nao.ac.jp), [2]Geographical Survey Institute (1 Kitasato, Tsukuba Ibaraki, 305-0811, Japan) , [3]Japan Aerospace Explolation Agency (2-1-1 Sengen, Tsukuba Ibaraki, 305-8505, Japan), [4]German Aerospace Center (Rutherfordstraße 2, 12489 Berlin, Germany), [5]Ohio State Univ. (275 Mendenhall Lab., Columbus, Ohio 43210, USA).

Introduction: The laser altimeter (LALT) onboard Japanese lunar explorer KAGUYA (SELENE) launched on 14 September, 2007 from Tanegashima Space Center (JAXA) is designed to perform the topography of the Moon from the altitude of 100 km [1]. LALT transmits Cr doped Nd:YAG laser pulses at 1 Hz to measure the distance from the spacecraft to the surface of the Moon. The nominal observation phase began on 30 December, 2007 and the number of geolocated points over the entire lunar surface is about 1.1×10^7 as of 30 November, 2008. A global topographic map of the Moon with a spatial resolution less than 0.5° has been created using LALT data. This map reveals much more precise and realistic topographic details for scales less than a few hundred km than in the previous global topographic model. The preliminary version of the maps in several kinds of projection using data from 7 to 20 January, 2008, have been opened to the public since 9 April, 2008, from Geographical Survey Institute of Japan (http://gisstar.gsi.go.jp/selene/). They are also downloadable from KAGUYA Image Gallery (JAXA; http://wms. selene.jaxa.jp/selene_viewer/index_e.html) and from RISE project in National Astronomical Observatory of Japan (http://risewww. mtk.nao.ac. jp/).

Topographic Mapping: The radial topographic error is estimated to be ± 4.1 m (1 σ), where the range shift (<12m) caused by the distortion of the bounced laser signals due to the sloped and/or rough target terrain is dominant and incorporated to be 4 m (1 σ). The horizontal topographic error is estimated to be ± 77 m (1 σ), where the orbit and pointing errors are the principal error sources and incorporated in the root sum square sense. The cross track spacing is less than 0.5°. Within both polar regions for more than 89° in latitude, 50 or 60 thousands range data have been obtained. The mean number density is 1/ (220 or 240) m^2 with the largest gap about 2*2 km^2.

Lunar Figure and Topography: The new lunar topographic map (Fig. 1) shows that the highest point on the Moon is located in the south rim of the Dirichlet-Jackson Basin; (-158.64°E, 5.44°N, 10.75 km). The lowest point is inside of the small crater in the Antoniadi crater; (-172.58°E, 70.43°S, -9.06 km).

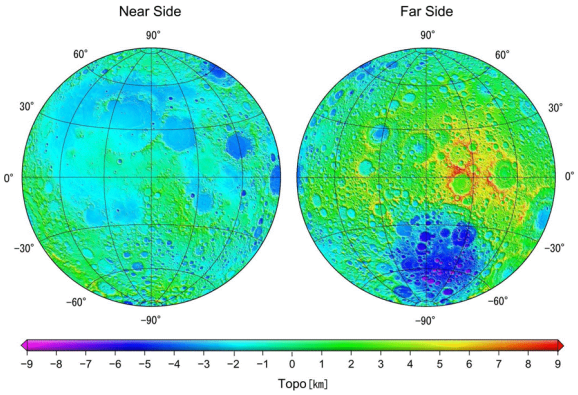

Fig. 1 Lunar shaded topographic map using LALT data (~30 June, 2008) by Lambert equal area projection.

The height difference is confirmed to reach almost 20 km. The second and third lowest points are also in the small crater in the Bellingshousen and Lemaitre F crater; the heights are -8.86km and -8.71km respectively. The lowest three points are all in the SPA basin. The reference sphere whose radius is 1737.4 km is centered on the lunar COM (center of mass) and set to

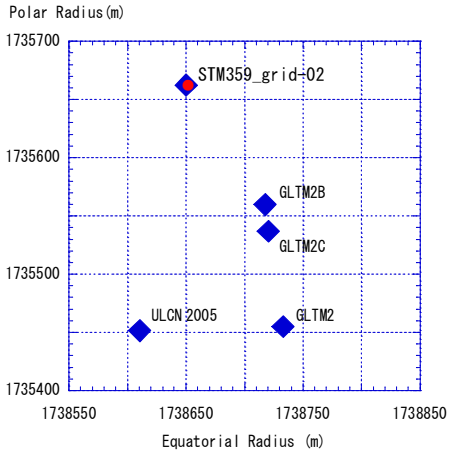

Fig. 2 Lunar equatorial and polar radius derive from STM359_grid-02 and the previous lunar global topographic models.

the mean Earth / polar axis lunar coordinates [2]. The mean radius of the Moon is estimated 1737.15 ± 0.01 km from the coefficient C_{00} of the new lunar spherical

harmonic topographic model (STM359_grid-02) derived from LALT observation. The COM-COF (Center of Mass - Center of Figure) offset is derived from the C_{1m} (m=0, 1) as (–1.772, –0.731, 0.239) km along three axes in the mean Earth / polar axis coordinates or 1.93 km in total. The direction of the COM-COF vector is displaced 22.41° east from the prime meridian and the 7.10° north from the equator on the far side. This is slightly north east of the highest elevation point of the Moon. The polar and mean equatorial radii are derived to be 1735.66 km and 1738.64 km respectively from the lunar mean radius (1737.15 km) and C_{20} coefficient. The polar flattening is thus obtained to be 1/581.899 from the two radii (Fig. 2).

STM359_grid-02 shows the amplitude of the power spectrum of the lunar topography is larger than that of the previous model at >30 degree (half wavelength scale about 180 km) and that the spectrum is almost flat between 30 and 70 degrees [3]. The global correlation and admittance spectra calculated from the new topography and gravity model (SGM90d) show their abrupt increase around the 30 degree (Fig. 3). These characteristics may indicate that the lunar topography for the scale more than about 180 km is maintained at least partly by the isostatic compensation on the Moho interface while the topography smaller than 180km is supported mainly by the crustal rigidity.

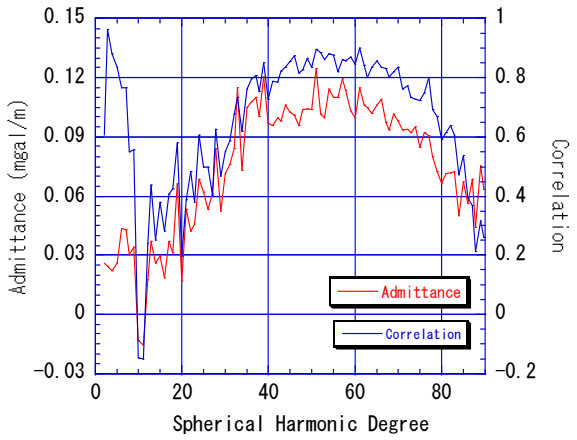

Fig. 3 Lunar Global correlation and admittance spectra.

Polar illumination: The first lunar polar topographic map has been derived by LALT altimetry with the complete coverage. Owing to orbit convergence around the poles, we can confirm craters clearly at least down to 2 or 3 km across. The topography is clearly rougher in the south polar region than in the north due to its position near the rim of SPA basin. Based on the LALT topographic map, Noda *et al.* [4] calculated the solar illumination condition around both polar regions (> 85°) for 2000 days (5.5 yr), showing that the sun lit rate is 89 % or 86 % at most for the north or south region respectively. The permanent shadow area (> 87.5°) is 844 km^2 or 2751 km^2 for the north or south respectively, resulting from the difference of the topographic roughness in the two polar regions.

Acknowledgements: SHTOOLS2.4 [5] is used for the calculation of the STM359_grid-02 model and the global correlation and admittance spectra.

References: [1] Araki H. *et al*. (2008) *Adv. Space Res.*, **42,** 317-322. [2] Seidelmann P. K. *et al*. (2007) *Celestial Mech. Dyn. Astr.*, **98**, 155-180. [3] Araki H. *et al*., Submitted to *Science*. [4] Noda H. *et al*. (2008) *GRL*, **35**, L24203. [5] Wieczorek M. (2007) http://www.ipgp.jussieu.fr/~wieczor/SHTOOLS/SHTOOLS.html.